

****FULL TITLE****

*ASP Conference Series, Vol. **VOLUME**, **YEAR OF PUBLICATION***

****NAMES OF EDITORS****

The Evolution of Galaxy Dust Properties for $1 < z < 2.5$

Stefan Noll, Daniele Pierini, Maurilio Pannella, and Sandra Savaglio

*Max-Planck-Institut für extraterrestrische Physik, Giessenbachstr.,
85748 Garching, Germany*

Abstract. Fundamental properties of the extinction curve, like the slope in the rest-frame UV and the presence/absence of a broad absorption excess centred at 2175 Å (the UV bump), are investigated for a sample of 108 massive, star-forming galaxies at $1 < z < 2.5$, selected from the FDF Spectroscopic Survey, the K20 survey, and the GDDS. These characteristics are constrained from a parametric description of the UV spectral energy distribution of a galaxy. It turns out that the sample galaxies host dust producing extinction curves with properties in between those of the Small and Large Magellanic Clouds (SMC and LMC, respectively). LMC-like extinction curves, which exhibit a UV bump, are mainly found among highly-reddened, UV-ultraluminous galaxies at $z \sim 2.4$ and highly-reddened, near-IR-bright, star-forming galaxies at $z \sim 1.2$. We discuss star-formation rates, total stellar masses, the morphology, and the chemical properties of our sample galaxies with respect to possible explanations for the different extinction curves.

1. Introduction

Nearby starburst galaxies probably contain dust with an extinction curve lacking a broad bump centred at 2175 Å (Calzetti et al. 1994). This is typical of the Small Magellanic Cloud (SMC), whose harsh environments (i.e. strong radiation fields and shocks) and/or low metallicity do not allow a large presence of those grains that are proposed as the carriers of the UV bump (Gordon et al. 2003). However, the supershell region surrounding 30 Dor in the Large Magellanic Cloud (LMC) contains such carriers, which are ubiquitous in the diffuse interstellar medium (ISM) of the Milky Way.

Are there star-forming galaxies at high redshift exhibiting the dust absorption feature at 2175 Å in their spectra? While for most objects the answer to this question is no or at least doubtful (e.g., Vihj et al. 2003; Wang et al. 2004; York et al. 2006), Noll & Pierini (2005) find that the majority of reddened UV-luminous galaxies at $2 < z < 2.5$ show clear evidence of the 2175 Å bump. These galaxies seem to experience strong dust reddening (Noll et al. 2004) and seem to be massive and metal rich (Mehlert et al. 2002; Daddi et al. 2004; Shapley et al. 2004). In order to investigate whether the carriers of the 2175 Å feature exist in other galaxy populations at different cosmic times, we extend our analysis of rest-frame UV spectra to additional UV-luminous and massive galaxies at $1 < z < 2.5$ (Noll et al., in prep.).

2. The Spectroscopic Sample

In addition to the 34 galaxies at $2 < z < 2.5$ with $R_{\text{Vega}} < 24.8$ already studied by Noll & Pierini (2005), we select 32 $1 < z < 2$ objects with $R < 24$ from the *I*-limited FORS Deep Field (FDF) Spectroscopic Survey (Noll et al. 2004). This sample is complemented by 34 star-forming galaxies at $1 < z < 2.3$ selected from the spectroscopic catalogue of the K20 Survey in the Chandra Deep Field South and a field around the quasar 0055-2659 (Cimatti et al. 2002; Mignoli et al. 2005). Besides $K_s < 20$ all objects but two have $R < 24$. Finally, we consider eight star-forming galaxies at $1.5 < z < 2.3$ from the *I* and *K*-limited Gemini Deep Deep Survey (GDDS, Abraham et al. 2004), all with $R < 24.7$ and $K_s \lesssim 21.0$.

3. Analysis

In order to study the UV spectral energy distributions of our sample galaxies we use parameters based on power-law fits of the form $f(\lambda) \propto \lambda^\gamma$ to sub-regions of the UV continuum. The UV-bump indicator $\gamma_{34} = \gamma_3 - \gamma_4$ (Noll & Pierini 2005) is based on continuum slope measurements in the wavelength ranges $1900 - 2175 \text{ \AA}$ (γ_3) and $2175 - 2500 \text{ \AA}$ (γ_4), respectively. The “classical” UV reddening measure β is taken for $1250 - 1750 \text{ \AA}$ (Calzetti et al. 1994; Leitherer et al. 2002). Due to a different accessible wavelength range we take β_b as a reddening measure for galaxies at $z < 2$. This parameter is derived at $1750 - 2600 \text{ \AA}$ excluding $1950 - 2400 \text{ \AA}$, i.e. the range of the 2175 \AA feature. Wavelength regions affected by strong spectral lines are also excluded from the fitting procedure for all parameters (see Calzetti et al. 1994; Noll & Pierini 2005).

4. Results

Fig. 1 shows the UV-bump indicator γ_{34} versus redshift for our spectroscopic sample of 108 actively star-forming galaxies at $1 < z < 2.5$. Galaxies with strong 2175 \AA features, i.e. $\gamma_{34} < -2$, are mainly found at $2.3 < z < 2.5$ (38% of the FDF galaxies in this redshift range) and $1 < z < 1.5$. Considering that about 29% of the objects in the whole photometric FDF sample at $1 < z < 1.5$ with $R < 24$ show $K_s < 20$ (Heidt et al. 2003; Gabasch et al. 2004), we can combine the FDF and K20 samples and estimate that about 25% of the $1 < z < 1.5$ galaxies with $R < 24$ have $\gamma_{34} < -2$. 87% of these galaxies exhibit $K_s < 20$. Among the $1 < z < 1.5$ galaxies, only objects with $z < 1.2$ show very strong 2175 \AA features as indicated by $\gamma_{34} < -5$. At $1.5 < z < 2.2$ only two out of 26 galaxies indicate $\gamma_{34} < -2$. In one case the redshift is uncertain and in the other case $R = 24.4$, which does not fulfil the $R < 24$ criterion. The latter object suggests that $1.5 < z < 2.2$ galaxies with relatively strong UV bumps could pop up just at fainter luminosities than covered by the selection limit $R = 24$ (see Fig. 2). Most sample galaxies with $\gamma_{34} < -2$ at $z \sim 1.1$ would not have been detected, if they had been at $1.5 < z < 2.2$. On the other hand, there seems to be a real lack of high-luminosity objects with $\gamma_{34} < -2$ at these redshifts, since objects like those found at $z \sim 2.4$ should be easily detectable at $1.5 < z < 2.2$ (see Fig. 2).

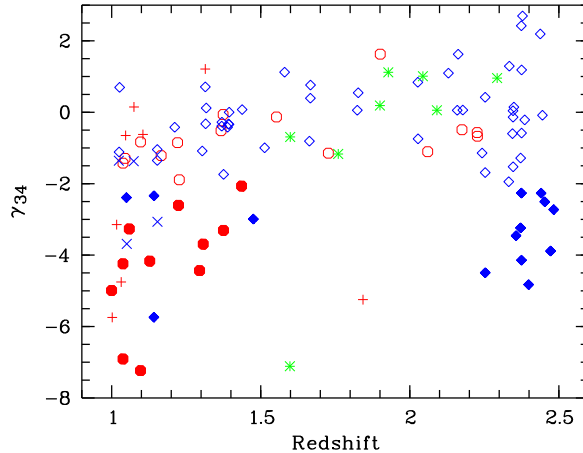


Figure 1. The UV-bump indicator γ_{34} versus redshift for 108 actively star-forming galaxies at $1 < z < 2.5$ selected from the FDF Spectroscopic Survey (lozenges and \times), the K20 Survey (circles and $+$), and the GDDS (asterisks). Galaxies without a UV-continuum slope derivation (\times , $+$, and asterisks) are no more considered in Figs. 2 and 3.

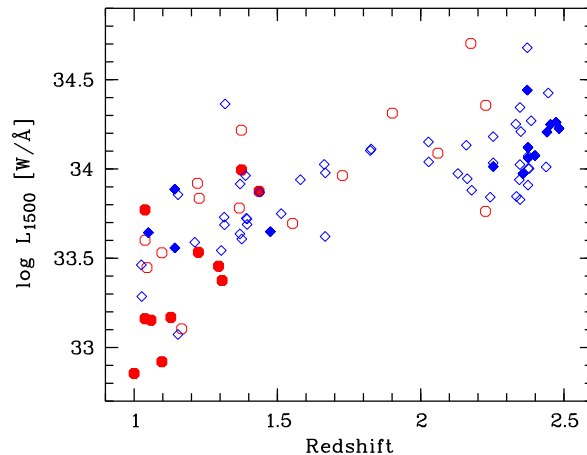


Figure 2. Luminosity at 1500 \AA versus redshift for 88 galaxies of the FDF Spectroscopic Survey (lozenges) and the K20 survey (circles). Galaxies with $\gamma_{34} < -2$ (i.e. with a prominent 2175 \AA feature) are marked by filled symbols.

Noll & Pierini (2005) find that the UV continua of UV-luminous galaxies at $2 < z < 2.5$ suggest effective extinction curves ranging from those typical of the SMC to those typical of the LMC. Fig. 3 shows that this also seems to be true for galaxies at $1 < z < 1.5$. The average γ_{34} decreases with increasing UV-reddening parameter β_b as expected for extinction curves showing a significant UV bump. For $\beta_b < -1.5$ the K_s -weighted average $\langle \gamma_{34} \rangle = -0.44 \pm 0.18$, while for $\beta_b > -0.5$ $\langle \gamma_{34} \rangle = -3.48 \pm 0.51$.

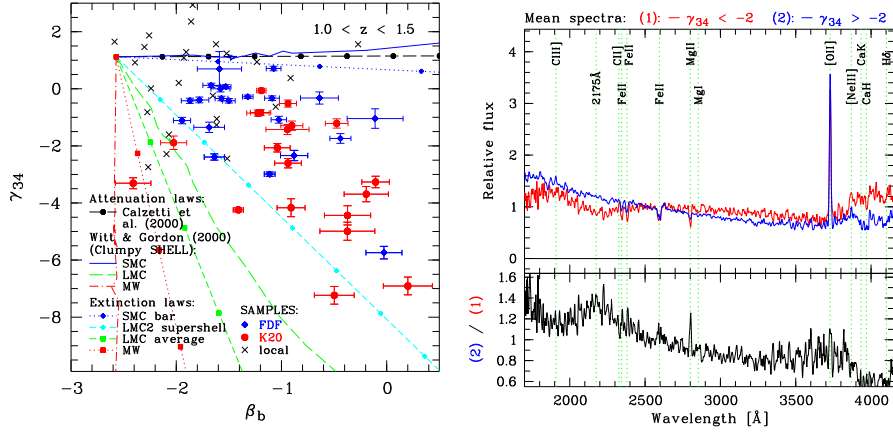


Figure 3. *Left:* The UV-bump indicator γ_{34} versus the reddening measure β_b for our $1 < z < 2.5$ FDF (lozenges), and K20 galaxies (circles), and a comparison sample of 24 local starburst galaxies (crosses) observed with IUE (see Noll & Pierini 2005). The diagram also shows different dust attenuation models (see legend) for a Maraston (2005) stellar population synthesis model with Salpeter IMF, continuous SF, an age of 100 Myr, and solar metallicity. The symbols are plotted in intervals of $\Delta E_{B-V} = 0.1$. *Right:* Comparison of K_s -weighted composite spectra of our $1 < z < 1.5$ galaxies exhibiting $\gamma_{34} > -2$ (blue or dark grey) and $\gamma_{34} < -2$ (red or grey), respectively (*top*). The ratio of both composites, normalised at $2400 - 2570 \text{ \AA}$, is also shown (*bottom*).

Fig. 3 also shows a comparison of the K_s -weighted composite spectra of $1 < z < 1.5$ galaxies with $R < 24$ having a weak ($\gamma_{34} > -2$) and a strong ($\gamma_{34} < -2$) 2175 \AA absorption feature, respectively. The presence of the feature in the more reddened composite with $\gamma_{34} < -2$ is evident. Moreover, as indicated by the stronger Balmer/ 4000 \AA break (e.g., Balogh et al. 1999) this spectrum seems to have an important contribution of an intermediate-age stellar population (i.e. $10^2 - 10^3 \text{ Myr}$) and/or to show an about three times older stellar population than the composite of galaxies with weak or absent UV bump. Finally, Fig. 3 exhibits a stronger Mg II absorption in relation to the strength of the Fe II absorption for the composite of the galaxies with $\gamma_{34} < -2$. This finding is also consistent with the above age estimates, whether the nature of the Mg II absorption is interstellar only (chemical enrichment of Mg in the ISM) or, also, partly stellar (composition of the stellar population).

From fits (the UV-bump range excluded) of the spectra of our sample galaxies with stellar population synthesis models of Maraston (2005) reddened using the “Calzetti law” (Calzetti et al. 2000) we obtain average star-formation rates (SFRs) for different subsamples as indicated in Fig. 4. For both redshift ranges the “red” subsamples (i.e. $\beta < -0.4$ for $2 < z < 2.5$ and $\beta_b < -1.5$ for $1 < z < 1.5$) have higher average SFRs than the “blue” subsamples due to larger dust reddening. Moreover, the $1 < z < 1.5$ galaxies exhibit lower SFRs (by a factor of 2 to 4) than the $2 < z < 2.5$ galaxies. For the total stellar masses (Drory et al. 2005; Pannella et al. 2006) Fig. 4 shows similar trends as those

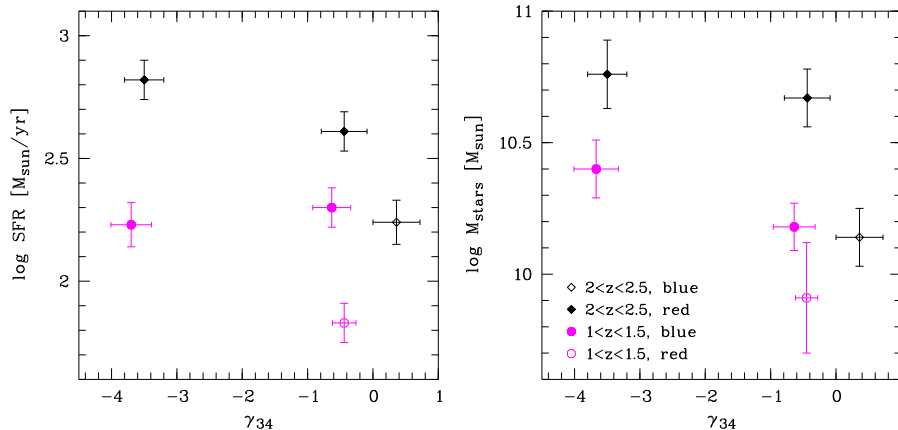


Figure 4. SFR (*left*) and total stellar mass (*right*) versus the UV-bump proxy γ_{34} for six subsamples. Lozenges and circles indicate the FDF $2 < z < 2.5$ and the FDF+K20 $1 < z < 1.5$ galaxies, respectively. Open symbols mark the subsamples with low reddening ($\beta < -0.4$; $\beta_b < -1.5$), while the highly reddened galaxies are represented by filled symbols. The errors indicated are mean errors.

for the SFR. Bluer and lower-redshift galaxies tend to have lower masses. The latter trend is in agreement with the “downsizing” scenario (Cowie et al. 1996). Estimates of the metallicity using different spectral features for $2 < z < 2.5$ (Mehlert et al. 2002, 2005) and the mass-metallicity relation of Savaglio et al. (2005) for $1 < z < 1.5$ (because of the lack of suitable spectral features in the accessible wavelength range) suggest typical values close to solar for at least the red subsamples in both redshift ranges. Hence, for constant UV-continuum reddening SFR, mass, and metallicity do not obviously correlate with the strength of the UV bump.

We analyse the morphology of our sample galaxies from red Hubble ACS images using GIM2D (Simard et al. 1999) for a PSF-convolved Sérsic-profile fitting and the CAS parametrisation of Conselice et al. (2000, 2003). For $1 < z < 1.5$ the red galaxies tend to have larger radii, and lower Sérsic and concentration indices than the blue galaxies. The latter two parameters also seem to be lower for red galaxies with stronger UV bumps. For the Sérsic index, e.g., we find 0.54 ± 0.25 ($\beta_b > -1.5$ and $\gamma_{34} < -2$) and 0.98 ± 0.23 ($\beta_b > -1.5$ and $\gamma_{34} > -2$), respectively. The parameters measured and a visual inspection of the images imply that particularly $1 < z < 1.5$ galaxies with relatively strong UV bumps are often disc galaxies. At $2 < z < 2.5$ there are obviously similar trends in the morphological parameters (at least for the relation between blue and red galaxies), but less significant. A difference is the higher “clumpiness” of the light distributions of the red galaxy sample. From a visual inspection of these galaxies we learn that at least half of the objects exhibit multiple components due to a patchy distribution of young stars and gas and/or (major) merger events.

5. Conclusions

We have constrained properties of the extinction curves for 108 UV-luminous galaxies at $1 < z < 2.5$. The strongest evidence for the dust absorption feature at 2175 Å (which can be as strong as in the LMC) comes from objects around $z \sim 1.1$ and $z \sim 2.4$.

At $2 < z < 2.5$ galaxies with relatively strong UV bumps are highly dust-enshrouded, i.e. there is a high neutral clouds' covering fraction in the direction towards the observer (as suggested by the study of strong interstellar UV absorption lines; Noll & Pierini 2005). This implies that the carriers of the 2175 Å feature are protected from the strong and hard radiation fields and/or shocks in these ultraluminous galaxies by dust self-shielding due to high dust column densities. At $1 < z < 1.5$ the galaxies with relatively strong UV bumps are less massive, show lower SFRs, have similar sizes, contain a relatively high fraction of intermediate-age stars (including carbonaceous-dust producing AGB stars), and tend to be disc galaxies. Lower SFR densities could mean that the carriers of the 2175 Å feature are exposed to less harsh conditions in the ISM, which can ease the need for self-shielding.

Acknowledgments. This research was supported by the German Science Foundation (DFG, SFB 375).

References

- Abraham, R.G., Glazebrook, K., McCarthy, P.J., et al. 2004, *AJ*, 127, 2455
- Balogh, M.L., Morris, S.L., Yee, H.K.C., et al. 1999, *ApJ*, 527, 54
- Calzetti, D., Kinney, A.L., & Storchi-Bergmann, T. 1994, *ApJ*, 429, 582
- Calzetti, D., Armus, L., Bohlin, R.C., et al. 2000, *ApJ*, 533, 682
- Cimatti, A., Mignoli, M., Daddi, E., et al. 2002, *A&A*, 392, 395
- Conselice, C.J., Bershad, M.A., & Jangren, A. 2000, *ApJ*, 529, 886
- Conselice, C.J., Bershad, M.A., Dickinson, M., et al. 2003, *AJ*, 126, 1183
- Cowie, L.L., Songaila, A., Hu, E.M., et al. 1996, *AJ*, 112, 839
- Daddi, E., Cimatti, A., Renzini, A., et al. 2004, *ApJ*, 600, L127
- Drory, N., Salvato, M., Gabasch, A., et al. 2005, *ApJ*, 619, L131
- Gabasch, A., Bender, R., Seitz, S., et al. 2004, *A&A*, 421, 41
- Gordon, K.D., Clayton, G.C., Misselt, K.A., et al. 2003, *ApJ*, 594, 279
- Heidt, J., Appenzeller, I., Gabasch, A., et al. 2003, *A&A*, 398, 49
- Leitherer, C., Li, I.-H., Calzetti, D., et al. 2002, *ApJS*, 140, 303
- Maraston, C. 2005, *MNRAS*, 362, 799
- Mehlert, D., Noll, S., Appenzeller, I., et al. 2002, *A&A*, 393, 809
- Mehlert, D., Tapken, C., Appenzeller, I., et al. 2006, *A&A*, 455, 835
- Mignoli, M., Cimatti, A., Zamorani, G., et al. 2005, *A&A*, 437, 883
- Noll, S., Mehlert, D., Appenzeller, I., et al. 2004, *A&A*, 418, 885
- Noll, S., & Pierini, D. 2005, *A&A*, 444, 137
- Pannella, M., Hopp, U., Saglia, R.P., et al. 2006, *ApJ*, 639, L1
- Savaglio, S., Glazebrook, K., Le Borgne, D., et al. 2005, *ApJ*, 635, 260
- Shapley, A.E., Erb, D.K., Pettini, M., et al. 2004, *ApJ*, 612, 108
- Simard, L., Koo, D.C., Faber, S.M., et al. 1999, *ApJ*, 519, 563
- Vijh, U.P., Witt, A.N., & Gordon, K.D. 2003, *ApJ*, 587, 533
- Wang, J., Hall, P.B., Ge, J., et al. 2004, *ApJ*, 609, 589
- Witt, A.N., & Gordon, K.D. 2000, *ApJ*, 528, 799
- York, D.G., Khare, P., Vanden Berk, D., et al. 2006, *MNRAS*, 367, 945